

Thermoelectric properties of doped BaHfO₃

Chandra Kr. Dixit, K. C. Bhamu, and Ramesh Sharma

Citation: [AIP Conference Proceedings](#) **1728**, 020125 (2016); doi: 10.1063/1.4946176

View online: <http://dx.doi.org/10.1063/1.4946176>

View Table of Contents: <http://scitation.aip.org/content/aip/proceeding/aipcp/1728?ver=pdfcov>

Published by the [AIP Publishing](#)

Articles you may be interested in

[Improvement in J_c performance below liquid nitrogen temperature for SmBa₂Cu₃O_y superconducting films with BaHfO₃ nano-rods controlled by low-temperature growth](#)

APL Mater. **4**, 016102 (2016); 10.1063/1.4939182

[Fe modified BaTiO₃: Influence of doping on ferroelectric property](#)

AIP Conf. Proc. **1665**, 040018 (2015); 10.1063/1.4917631

[Influence of excess SrO on the thermoelectric properties of heavily doped SrTiO₃ ceramics](#)

Appl. Phys. Lett. **102**, 183905 (2013); 10.1063/1.4804372

[Thermoelectric properties of SnO₂-based ceramics doped with Nd, Hf or Bi](#)

AIP Conf. Proc. **1449**, 327 (2012); 10.1063/1.4731563

[Effects of elemental doping on the thermoelectric power of the thallium based superconductor Tl₂Ba₂Ca₂Cu₃O_{10-δ}](#)

AIP Conf. Proc. **316**, 119 (1994); 10.1063/1.46799

Thermoelectric Properties Of Doped BaHfO₃

*Chandra Kr. Dixit^a K.C Bhamu^b and *Ramesh Sharma^c

^a*Dept. of Physics, Dr.Shakuntala Misra National Rehabilitation University, Lucknow-229001, U.P India.*

^b*Department of Physics, Goa University, Goa-403 206,India*

^c*Dept. of Physics, Feroze Gandhi Institute of Engineering & Technology, Raebareli-229001, U.P India*

Corresponding author: *ckparadise@gmail.com, *sharmarameshfgiet@gmail.com

Abstract. We have studied the structural stability, electronic structure, optical properties and thermoelectric properties of doped BaHfO₃ by full potential linearized augmented plane wave (FP-LAPW) method. The electronic structure of BaHfO₃ doped with Sr shows enhances the indirect band gaps of 3.53 eV, 3.58 eV. The charge density plots show strong ionic bonding in Ba-Hf, and ionic and covalent bonding between Hf and O. Calculations of the optical spectra, viz., the dielectric function, refractive index and extinction coefficient are performed for the energy range are calculated and analyzed. Thermoelectric properties of semi conducting are also reported first time. The doped BaHfO₃ is approximately wide band gap semiconductor with the large p-type Seebeck coefficient. The power factor of BaHfO₃ is increased with Sr doping, decreases because of low electrical resistivity and thermal conductivity.

INTRODUCTION

As a result of a raising demand involving renewable energy, thermoelectric materials nowadays usually are attracting very much attention since they directly change thermal energy into electrical energy. For example, thermoelectric oxides usually are interesting because of the low producing costs, environmentally friendly, availability within nature, in addition to high support temperatures, high service temperatures. BaHfO₃, cubic perovskite which find wide range of applications such as special interest for memory, ferroelectricity semi conductivity, logic, memory storage capacitors and thermoelectricity, passive microelectronic applications [1-4]. Yangthaisong et al. investigated the electronic structure and lattice vibrational properties of BaHfO₃ by screened exchange local density approximation (sX-LDA) [5]. Ohta et.al. measured thermoelectric properties of heavily La/Nb-doped SrTiO₃ at high temperature and have found ZT values of 0.27 and 0.37 at 1000 K for 20% doping respectively [6-7]. Liu et al. studied the mechanical, electronic, chemical bonding and optical properties of cubic BaHfO₃ by plane-wave ultra soft pseudo-potential method based on the density-functional theory (DFT) [8]. Earlier work on to enhance the thermo power involving doped SrTiO₃ different atomic substitutions and defects are researched. In this work, BaHfO₃ is a semiconductor we focus on the Sr, doped analog and systematically study their structural, electronic and transport properties using first-principles density-functional calculations.

METHODOLOGY

The structure of BaHfO₃ are calculated using the WIEN2K package, which is an implementation of the hybrid full potential linear augmented plane wave method (GGA) within the density-functional theory (DFT). The atomic sphere radii R_{mt} are chosen to be 2.43, 1.73, 1.75 and 1.64 a.u. for Ba, Sr, Hf and O atoms, respectively. The convergence parameter RK_{max} ($R_{mt} \times K_{max}$, where K_{max} is the plane wave cut-off and R_{mt} represents the smallest among all atomic sphere radii), which determines the matrix size in these calculations, is set to be 7.0. The self-consistent calculations are carried out with a total energy convergence tolerance of less than 0.1mRy. We have used 1000 k -points in the entire Brillouin zone. We assume that BaSrHfO₃ has a similar structure to BaHfO₃ using Sr, as a substitute for Hf. The transport properties have been calculated using semi-classical Boltzmann theory as implemented in the BoltzTraP interfaced program with Wien2k [9,10]. The lattice parameters and other properties are summarized in Table 1.

RESULT & DISCUSSION

BaHfO₃ ideal cubic perovskite structure with space group Pm3m. The lattice sites remain in the ideal cubic perovskite positions with Ba in (0,0,0), Hf in (1/2,1/2,1/2) and O in (1/2,1/2,0). The energy band structure and densities of states (DOSs) of BaHfO₃ are shown in Figs. 1. The energy band structure is calculated along the way that contains the highest number of high symmetry points of the Brillouin zone. The top of the valence bands (VBs) and the bottom of conduction bands (CBs) are composed of O 2*p* and Ba 3*d* states, respectively. The VB maximum of BaSrHfO₃ is located at the Γ point, whereas the CB minimum is located at the Γ point, suggesting an indirect band gap. The VB show a slight shift to low energy, while the CB move to high energy. As a result, the energy gap of BaSrHfO₃ increases from 3.53 eV of BaHfO₃ to 3.58 eV. The bands between -10 and -12 eV mainly consist of O 2*s* states, and those at about -4 eV arise from Hf 3*d* states with a sharp peak due to its strong localization character. The Ba 6*s* states are located at about -10 eV with a bandwidth of 2 eV. Since the O 2*p* states have some admixture with the Ba, Sr and Hf *sp* states. In the VB region, the energy levels of Sr and Hf are clearly lower than that of Ba and O. This indicates that the hybridization of Ba-O is stronger than those of Sr-O and Hf-O. In the energy range from 3 eV to 10 eV, the bands are mainly derived from the Ba 6*p* states with some admixture from Sr and Hf *sp* states. From the analysis of DOS, it can be observed that there is strong orbital hybridization between the Hf 3*d* and O 2*p* states.

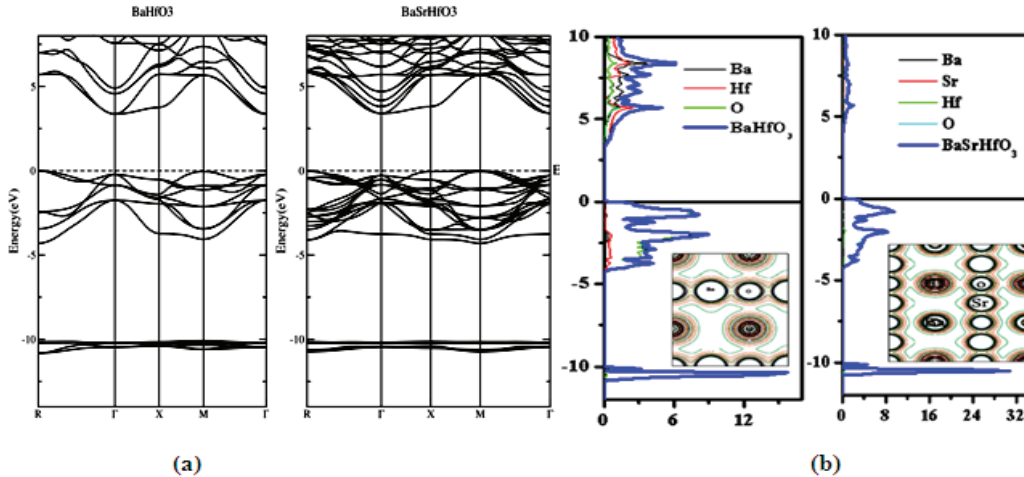


FIGURE 1. (a) Energy bands (b) Density of states

For, the contour plots of valence charge distribution have been calculated by considering the nature of the corresponding Ba-O, Hf-O, Sr-O and Hf-Sr bonds, which are displayed in the (1 1 1) plane. From Figs. 1(b), the given plots show a strong ionic but weak covalent character of Ba-O bond that can be attributed to the larger charge transfer among Ba and O atoms with very small contour extension. Figure 1(b) reveals the strong sharing and distribution of electrons along the Hf-O bond. As a result, their bond is strongly covalent nature is observed along the Sr-O and Hf-O bond.

The determination of the optical properties of a compound in the spectral range above its band gap plays an important role in the understanding of the nature of that material and also gives a clear picture of its applications in optoelectronic devices. The calculated imaginary part of dielectric function for BaHfO₃ and BaSrHfO₃ in the radiation range 0-12 eV are shown in Fig. 2 (a). Our analysis $\epsilon_2(\omega)$ curve shows that the threshold energy (the first critical point) of the dielectric function occurs at 2.05 and 1.27 eV for BaHfO₃ and BaSrHfO₃, respectively. These points give the threshold for direct optical transitions between the highest valence and the lowest conduction bands. It is known as the fundamental absorption edge. Beyond these points, the curve increases rapidly because the number of points contributing towards $\epsilon_2(\omega)$ increases abruptly. The main features in the spectrum of the real part $\epsilon(\omega)_1$ are a peak with a magnitude of 7.22, 7.70 at around 4.29 eV, a decrease between 5.76 and 9.57 eV, for BaHfO₃ and BaSrHfO₃ respectively. After which $\epsilon(\omega)_1$ becomes negative, and a minimum at around 10.56 eV, followed by a slow increase toward zero. The most important quantity is the zero frequency limit $\epsilon(0)_1$, which is the electronic part of the static dielectric constant and depends strongly on the band gap.

The efficiency of thermoelectric devices is determined by the dimensionless figure of merit, $zT = \sigma S^2 T / \kappa$, where σ is the electrical conductivity, S is the Seebeck coefficient, T is the temperature, and κ is the thermal conductivity. The latter comprises lattice (κ_{lattice}) and electronic (κ_{electron}) contributions, $\kappa_{\text{total}} = \kappa_{\text{lattice}} + \kappa_{\text{electron}}$. In order to achieve a high efficiency, the thermoelectric material, in general, should be a good electrical and poor thermal conductor and, at the same time, possess a high Seebeck coefficient. Fig.2 (b), shows the temperature dependence of the thermo power for BaHfO₃ and BaSrHfO₃ with p-type carrier concentration at fixed to 10^{19} cm^{-3} . High thermopower S is observed in p-type BaHfO₃ and BaSrHfO₃ over whole temperature range. Room temperature thermo powers are $267 \mu\text{V/K}$ and $127 \mu\text{V/K}$ for p-type BaHfO₃ and BaSrHfO₃, respectively. While in p-type both materials shows similar behavior. This value is quite similar to their iso-structural compounds like SrTiO₃. Previously reported pervoskites such as SrTiO₃, BaTiO₃ and PbTiO₃ have band-gaps around 3 eV (insulators) which is far from the visible region and Seebeck values are always high for large band gap materials. The electrical conductivity is very low, this results in small $S^2\sigma$ (Power factor) at low temperature, but after doping of Sr in BaHfO₃, the power factor of BaSrHfO₃ increases from room temperature. In our study, bandgap is around 3.5 eV which half of them and a moderate doping could make these materials as good candidate for optoelectronic and thermoelectric devices. The Seebeck coefficient of BaHfO₃ has high at room temperature in comparison to BaSrHfO₃ and gradually decreases at RT and both value of S is positive, suggesting that the holes to be the majority carriers. We have reported first time the ZT of Sr doped BaHfO₃ is decreases.

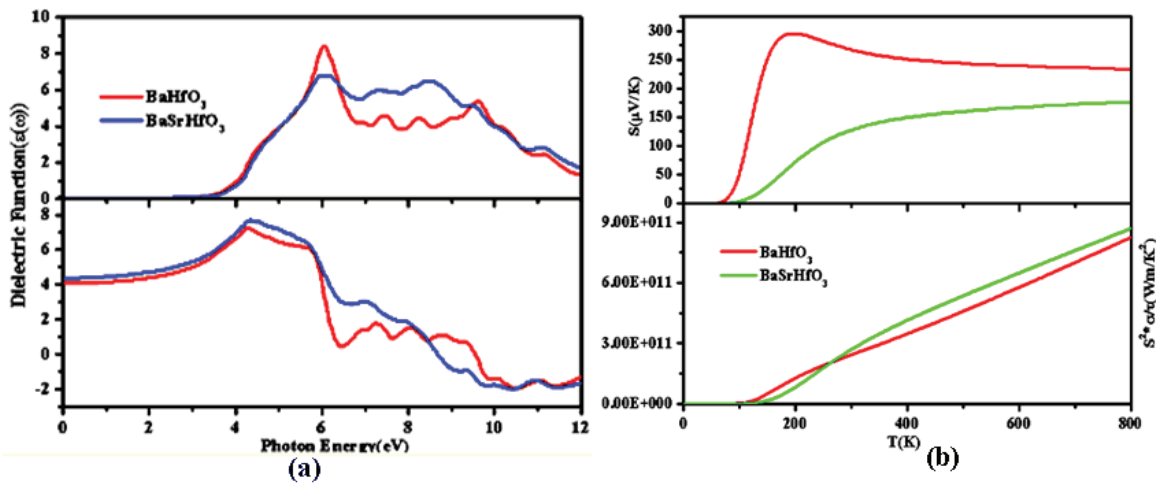


FIGURE 2. (a) Optical property (b) (c) Transport property

TABLE 1. Out parameters

Parameters	BaHfO ₃	BaSrHfO ₃
Band gap (eV)	3.53[Ref.5]	3.58
S ($\mu\text{V/K}$)	267	127
$R_H(10^{-8})(\text{m}^3/\text{C})$	2.10	4.07
ZT	0.81	0.43

SUMMARY

The electronic structure and thermoelectric properties are calculated for doped BaHfO₃. The calculated optimized structural parameters, band gaps are in good agreement with the experimental data. The band structure of BaSrHfO₃ shows the indirect band gap ($R-\Gamma=3.58\text{eV}$) semiconductors. The electronic structures of BaSrHfO₃ reveal that the top of a VB and the bottom of a CB are decided by O 2*p* and Ba 6*p* states, respectively. Furthermore, BaSrHfO₃ shows some covalent features which can reduce the total energy and help maintain the stability of the semiconductor property. High thermo power 267 $\mu\text{V/K}$ is observed in n-type BaHfO₃ as compared to BaSrHfO₃ ($S = 127 \mu\text{V/K}$) at room temperature. It is expected that the present study will provide better insight in understanding electronic as well as thermoelectric properties of these materials.

ACKNOWLEDGMENTS

One of the authors (KCB) is thankful to UGC, New Delhi for DS Kothari fellowship. We are also thankful to Peter Blaha for Wien2k code.

REFERENCES

1. C.B. Samantaray, H. Sim, H. Hwang, *J. Microelectron.* **36**, 725 (2005).
2. V.E. Henrich, *Rep. Prog. Phys.* **11**, 1481(1985).
3. H. Muta, K. Kurosaki, S. Yamanaka, *J. Alloys Compd.* **350**, 292(2003).
4. C B Samantaray and H Sim and H Hwang, *Phys. B: Condens. Matter*, **351**, 158(2004).
5. A. Yangthaisong *Phys. Let.A.* **377**, 927-931 (2013).
6. S. Ohta, T. Nomura, H. Ohta, M. Hirano, H. Hosono, and K. Koumoto, *Appl. Phys. Lett.* **87**, 092108 (2005).
7. S. Ohta, T. Nomura, H. Ohta, and K. Koumoto, *J. Appl. Phys.* **97**, 034106 (2005).
8. Q.J. Liu, Z.T. Liu, L.P. Feng, H. Tian *Phys. B: Cond. Mat.* **405**, 4032–4039 (2010).
9. P. Blaha, K. Schwarz, G. K. H. Madsen, D. Kvasnicka and J. Luitz, Wien2k, Vienna University of Technology, Vienna, Austria.
10. G.K.H Madsen and D.J Singh *Comp.Phys.Comm.***175**, 67-71 (2006).